Available online at www.sciencedirect.com
SCIENCE DIRECT
Journal of Solid State Chemistry 179 (2006) 1830–1841
JOURNAL OF SOLID STATE CHEMISTRY
www.elsevier.com/locate/jssc

# Incorporation of transition metals into Mg–Al layered double hydroxides: Coprecipitation of cations vs. their pre-complexation with an anionic chelator

Andrey Tsyganok, Abdelhamid Sayari*

*Centre for Catalysis Research and Innovation (CCRI), Department of Chemistry, University of Ottawa, 10 Marie Curie Street, Ottawa, Ont., Canada K1N 6N5*

Received 15 January 2006; received in revised form 14 March 2006; accepted 19 March 2006
Available online 28 March 2006

**Abstract**

A comparative study on two different methods for preparing Mg–Al layered double hydroxides (LDH) containing various divalent transition metals $M$ ($M$ = Co, Ni, Cu) has been carried out. The first (conventional) method involved coprecipitation of divalent metals $M$(II) with Mg(II) and Al(III) cations using carbonate under basic conditions. The second approach was based on the ability of transition metals to form stable anionic chelates with edta$^{4-}$ (edta$^{4-}$ = ethylenediaminetetraacetate) that were synthesized and further introduced into LDH by coprecipitation with Mg and Al. The synthesized LDHs were characterized by X-ray diffraction (XRD) and X-ray fluorescence (XRF) methods, thermogravimetry with mass-selective detection of decomposition products (TG-MSD), Fourier transform infrared (FTIR) and Raman spectroscopy techniques. The results obtained were discussed in terms of efficiency of transition metal incorporation into the LDH structure, thermal stability of materials and the ability of metal chelates to intercalate the interlayer space of Mg–Al LDH. Vibrational spectroscopy studies confirmed that the integrity of the metal chelates was preserved upon incorporation into the LDH.


*Keywords:* Layered double hydroxides; Coprecipitation; Transition metals; Edta; Chelation; Intercalation

## 1. Introduction

Layered double hydroxides (LDH) also known as anionic clays continue to attract the attention of chemists, material scientists and chemical engineers due to their unique physico-chemical properties and have found multiple applications [1,2]. Mg–Al LDH modified with various transition metals have been of particular interest in catalysis because they could serve as catalysts or precursors of catalysts for many industrially relevant reactions [3–6].

Traditionally, Mg–Al LDHs containing a guest transition metal have been synthesized via coprecipitation of metal cations under basic conditions (Fig. 1; left-hand side). In order to be inserted into the brucite-like layers of LDH, the metal should usually be di- or tri-valent and have an appropriate cation size. Carbonate has been commonly selected as the counter-ion and the products synthesized, denoted $M$(II)MgAl–$CO_3$ LDH, have a layered structure very similar to that of hydrotalcite $[Mg_6Al_2(OH)_{16}](CO_3)\cdot 4H_2O$ (MgAl–$CO_3$).

An alternative approach of incorporating a transition metal, for example Ni(II), into Mg–Al LDH has been reported recently [8,9]. It was based on the following two experimental observations: (i) the ability of Mg–Al LDH to incorporate and strongly retain multiple charged anions and (ii) the ability of Ni(II) to form with edta$^{4-}$ an anionic complex of 1:1 stoichiometry (Scheme 1) that is much more stable than the chelates of Mg(II) and Al(III) (Table 1). The latter suggested that coprecipitation of $Mg^{2+}$ and $Al^{3+}$ with pre-formed $[Ni(edta)]^{2-}$ might produce an LDH with potentially new properties (Fig. 1; right-hand side). The chelate was used in a 20-fold molar excess in order to suppress possible involvement into LDH of $NO_3^-$ (from the

*Corresponding author. Fax: +1 613 562 5170.
*E-mail address:* Abdel.Sayari@science.uottawa.ca (A. Sayari).

0022-4596/$ - see front matter © 2006 Elsevier Inc. All rights reserved.
doi:10.1016/j.jssc.2006.03.029

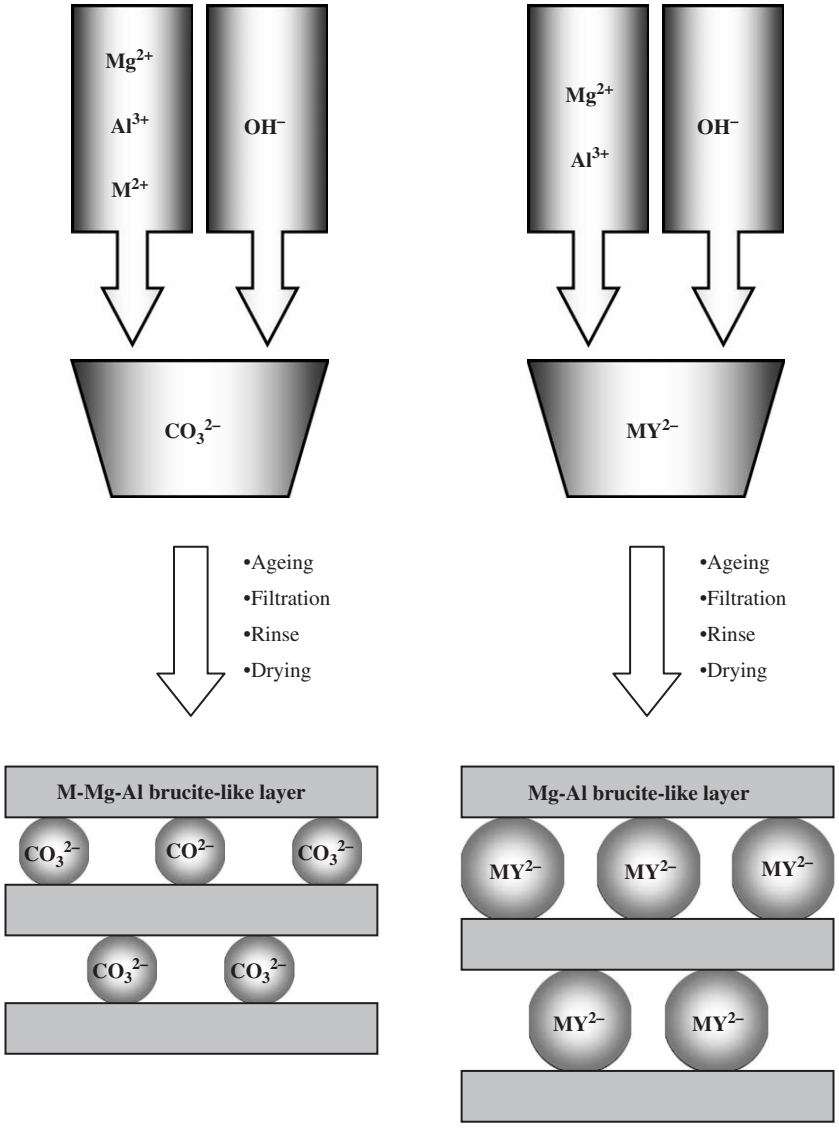


Fig. 1. Two ways for introducing transition metals $M$(II) into Mg–Al layered double hydroxides ($M$Y$^{2-}$ denotes the edta chelate of transition metal $M$(II)).

starting compounds) and $CO_3^{2-}$ that would originate from $CO_2$ in air.

The aim of the present work is to compare these two methods of LDH synthesis starting from solutions with the same molar amounts of metals. The difference between these two methods was in the starting state of transition metal to be introduced into the LDH. In the first (conventional) method, the metal was used in a cationic form ($M^{2+}$) and was coprecipitated with Mg(II) and Al(III). In the second technique, the transition metal was first complexed with edta$^{4-}$ into the chelate $[M(\text{edta})]^{2-}$, and such metal chelate was further coprecipitated with Mg(II) and Al(III). Additionally to Ni(II), we selected Co(II) and Cu(II) whose chelates are highly stable as well (Table 1). The phase structure of the synthesized solids was characterized by X-ray diffraction (XRD) and the metal content was measured by X-ray fluorescence. Thermogravimetry with mass-selective detection of decomposition products (TG-MSD) analysis of materials provided details of their thermal behavior. Fourier transform infrared (FTIR) and Raman spectroscopy studies revealed some structural features of anions involved into the synthesized LDH. To the best of our knowledge, there are no other characterization studies of Mg–Al LDH bearing $M$Y$^{2-}$ chelates using Raman spectroscopy.

## 2. Experimental section

### 2.1. Reagents and solvents

The nitrates of Mg(II), Al(III), Co(II), Ni(II) and Cu(II), the carbonate and hydroxide of sodium, and ethylenediaminetetraacetic acid were purchased from Aldrich. All compounds were of reagent grade and were used without additional purification treatment. The reference compounds were sodium edetates $Na_2Co(\text{edta})\cdot xH_2O$

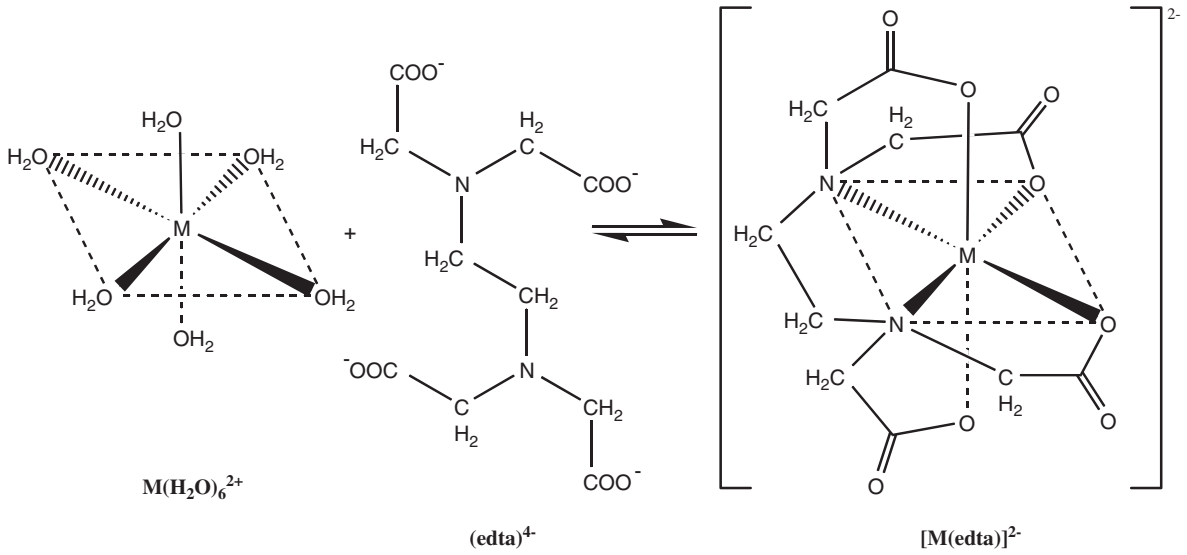


Scheme 1.

Table 1
Formation constants for edta chelates of various metals [7]

| Metal | Chelate | Log $K$ |
|---|---|---|
| Mg(II) | $[Mg(edta)]^{2-}$ | 8.64 |
| Al(III) | $[Al(edta)]^{-}$ | 16.11 |
| Co(II) | $[Co(edta)]^{2-}$ | 16.31 |
| Ni(II) | $[Ni(edta)]^{2-}$ | 18.56 |
| Cu(II) | $[Cu(edta)]^{2-}$ | 18.7 |

($Na_2CoY$), $Na_2Ni(edta)\cdot xH_2O$ ($Na_2NiY$) and $Na_2Cu(edta)\cdot xH_2O$ ($Na_2CuY$) of 98+% purity all that were purchased from TCI America Co. Distilled, deionized and degassed water was used throughout this work.

### 2.2. Synthesis of materials

Conventional synthesis of LDH by coprecipitation was carried out as follows. Sodium carbonate taken in a 2.5-fold excess to the amount required by stoichiometry was dissolved in 250 $cm^3$ of water. This solution was poured into a 3-neck, round-bottom flask and heated to 65 °C. The nitrates of Mg(II), Al(III) and a divalent transition metal $M$ taken in the amounts needed (Table 2) were placed into a conical flask and dissolved in 100 $cm^3$ of water. The solution thus obtained was added dropwise to a pre-heated $Na_2CO_3$ solution under vigorous stirring. The pH of the formed slurry was kept at 10.0 by adding a 1.0 M NaOH solution. After complete addition of the metal nitrate solution, the suspension was kept at 65 °C under stirring for 1 h and then left for ageing at the same temperature for 18 h without stirring. The precipitate was separated from solution by centrifuging at 2800 rpm speed for 5 min and was rinsed with three 500 $cm^3$ portions of water. The synthesized solids were dried in air at 90 °C for 48 h and stored in a desiccator at room temperature under vacuum.

The alternative technique involved pre-chelation of transition metals with edta. First, edta acid was converted into an anionic $edta^{4-}$ form by adding a known amount of a 1.0 M NaOH solution. Then the nitrate of the transition metal $M$(II) was added in an equimolar amount (Table 2) to form an $MY^{2-}$ complex and the solution pH was adjusted to 10.5 by adding NaOH solution. Afterward, the chelate solution was transferred into a 3-neck, round-bottom flask, diluted with water to a 250 $cm^3$ volume and heated to 65 °C. Then, the solution of Mg(II) and Al(III) nitrates in 100 $cm^3$ of water was added dropwise while keeping the pH of the slurry at 10.5 by addition of a 1.0 M NaOH solution. After complete addition of the (Mg(II) + Al(III)) solution, the suspension was stirred at 65 °C for an hour, followed by ageing at the same temperature without stirring for 18 h. Separation, rinsing, drying and storage of MgAl–$MY$ samples were carried out the same way as for conventionally synthesized LDHs.

### 2.3. Characterization techniques and procedures

Powder XRD patterns of all synthesized materials were recorded under air at room temperature using a Philips PW3020 diffractometer with a $Cu_{K\alpha}$ radiation source ($\lambda = 1.54056$ Å) at 45 kV and 40 mA. The patterns were acquired for $2\Theta$ range of 3–80° with a 0.033° $s^{-1}$ scan speed.

The Co, Ni and Cu contents in the materials synthesized were obtained by X-ray fluorescence using a Philips PW2400 XRF spectrometer previously calibrated for those elements using a concentration gradient of ultra-high purity oxides of Co, Ni and Cu in a $Mg_6Al_2O_9$ mixed oxide prepared from synthetic hydrotalcite by calcination in air at 500 °C for 16 h.

Table 2
Synthesis of transition metal-loaded Mg–Al double hydroxides

| Sample legend | Coprecipitating species (starting loadings in mmol) | Metal ratio measured by XRF in the samples | Suggested formula |
|---|---|---|---|
| $CoMgAl–CO_3$ | $Co^{2+}(20)$, $Mg^{2+}(120)$, $Al^{3+}(40)$, $CO_3^{2-}(50)$ | Co:Mg:Al 0.98:6:1.94 | $[Co_1Mg_6Al_2(OH)_{18}](CO_3)\cdot xH_2O$ |
| $NiMgAl–CO_3$ | $Ni^{2+}(20)$, $Mg^{2+}(120)$, $Al^{3+}(40)$, $CO_3^{2-}(50)$ | Ni:Mg:Al 0.94:6:1.98 | $[Ni_1Mg_6Al_2(OH)_{18}](CO_3)\cdot xH_2O$ |
| $CuMgAl–CO_3$ | $Cu^{2+}(20)$, $Mg^{2+}(120)$, $Al^{3+}(40)$, $CO_3^{2-}(50)$ | Cu:Mg:Al 1.04:6:1.97 | $[Cu_1Mg_6Al_2(OH)_{18}](CO_3)\cdot xH_2O$ |
| $MgAl–CO_3$ | $Mg^{2+}(120)$, $Al^{3+}(40)$, $CO_3^{2-}(50)$ | Mg:Al 6:1.98 | $[Mg_6Al_2(OH)_{16}](CO_3)\cdot xH_2O$ |
| MgAl–CoY | $Mg^{2+}(120)$, $Al^{3+}(40)$, $CoY^{2-}(20)$ | Co:Mg:Al 0.44:6:1.97 | $[Mg_6Al_2(OH)_{16}](CoY)_{0.44}(NO_3)_X(CO_3)_{(1.12-X)}\cdot yH_2O$ |
| MgAl–NiY | $Mg^{2+}(120)$, $Al^{3+}(40)$, $NiY^{2-}(20)$ | Ni:Mg:Al 0.47:6:1.98 | $[Mg_6Al_2(OH)_{16}](NiY)_{0.47}(NO_3)_X(CO_3)_{(1.06-X)}\cdot yH_2O$ |
| MgAl–CuY | $Mg^{2+}(120)$, $Al^{3+}(40)$, $CuY^{2-}(20)$ | Cu:Mg:Al 0.47:6:1.96 | $[Mg_6Al_2(OH)_{16}](CuY)_{0.47}(NO_3)_X(CO_3)_{(1.06-X)}\cdot yH_2O$ |

TG-MSD runs were carried out with a TA Instruments Q500 analyzer coupled to a Pfeiffer Thermostar mass-selective detector. During a typical run, the powdered samples (59–125 mg in loading) were first kept at 25 °C for 10 min and then heated to 1000 °C at a 10 °C $min^{-1}$ rate under a 100 $cm^3$ $min^{-1}$ flow of helium. The effluent gases were monitored by MSD for $H_2O$ (mass-to-charge ratio, $m/z = 18$), $CO_2$ ($m/z = 44$), CO ($m/z = 28$), NO ($m/z = 30$) and $CH_2$-fragments ($m/z = 14$).

FTIR and Raman spectra of solids were collected with a LabRam-IR HR800 system from HORIBA Jobin Yvon Co. This system consisted of a combination of a miniaturized IlluminatIR-interferometer from SensIR Technologies, Ltd. and a high-resolution dispersive Raman spectrometer equipped with a confocal Olympus microscope. Spectra acquisition and data processing were done using either GRAMS or LabSpec software. An attenuated total reflectance (ATR) objective was used for collecting FTIR spectra of samples. The powders were brought into direct contact with a ZnSe/diamond crystal of ATR, the contact efficiency being monitored via a real-time observation of IR spectrum. Once sufficient contact with sample was achieved, the collection of spectrum proceeded with 256 scans at a 4 $cm^{-1}$ resolution. For measuring Raman spectra, the powdered samples were irradiated with an Ar-ion laser light ($\lambda = 514.532$ nm) and the backscattered radiation passed through a 100× objective (numerical aperture 0.9), a specific notch filter for the rejection of the exciting line, a 200 μm confocal hole (i.e., spectrograph entrance slit) and then was detected by a charge-coupled device (CCD) camera. A grating with 1800 grooves per mm was used for high-resolution measurements. The spectra were collected with an integration time of 10 cycles by 5 s each.

## 3. Results

### 3.1. Powder X-ray diffraction

The XRD patterns for the current powdered materials are shown in Fig. 2. All materials synthesized by the traditional coprecipitation technique revealed patterns very similar to each other and to that of the reference hydrotalcite. The presence of three intense reflection peaks at $2\Theta$ 11.3, 22.6 and 34.4° indicated that the synthesized hydroxides were well crystallized and had a layered structure with a 3R layer stacking order akin to that of $MgAl–CO_3$. No change was observed in the $d_{[110]}$ parameter (1.53 Å), thus indicating that the average cation–cation distance in the brucite-like layers of the synthesized materials remained unaffected (Table 3).

The samples synthesized via preliminary chelation of transition metals with edta showed significantly different XRD patterns. The materials appeared to have lower crystallinity as they showed broader, less intense reflection peaks. For MgAl–NiY sample, two new peaks at $2\Theta$ 6.70 and 19.10° and a shoulder at 12.53° appeared. This

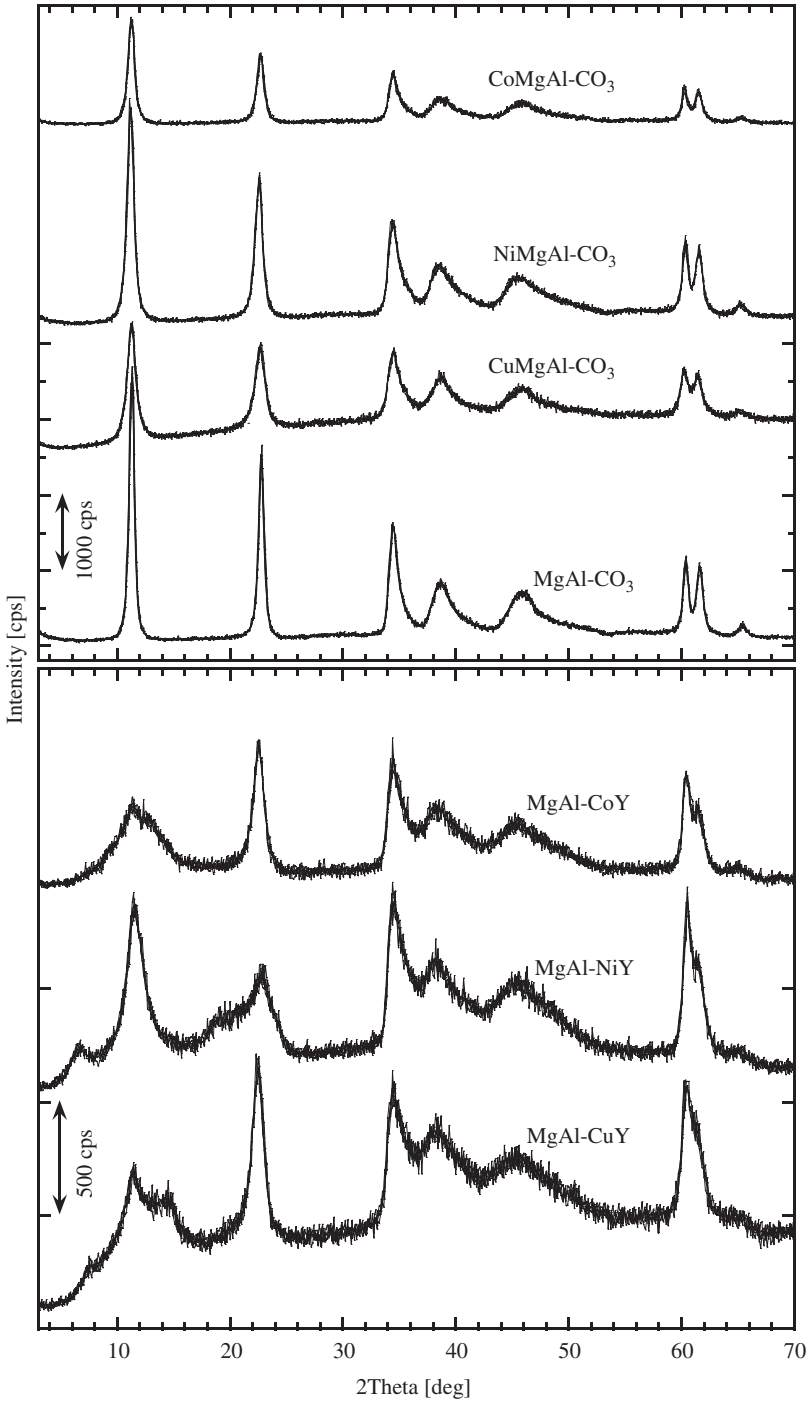


Fig. 2. Powder X-ray diffractograms for Mg–Al double hydroxides containing transition metals (the pattern of the reference MgAl–$CO_3$ hydrotalcite is shown for comparison).

indicated that a new LDH phase possibly having a 3R layer stacking order but with larger *d*-spacing was formed. This observation strongly suggested that $NiY^{2-}$ species intercalated the interlamellar space of Mg–Al LDH and resided there. A similar phenomenon was observed with MgAl–CuY LDH. Here two new peaks were observed at $2\Theta$ 7.25 and 14.55° that were attributed to reflections from [003] and [006] planes of a newly formed phase due to the LDH intercalation. However, it was more difficult to reach a firm conclusion about intercalation of Mg–Al LDH with a $CoY^{2-}$ species as it was not detected by the XRD method. The pattern recorded had a broad peak of low intensity at $2\Theta$ 11.35° possibly due to the reflection from [003] plane of the hydrotalcite-like phase but could also represent a superposition of neighboring reflection peaks.

Table 3
Powder X-ray diffraction of Mg–Al double hydroxides

| Material | 2Θ (°) | d (Å) | [h k l] |
|---|---|---|---|
| $CoMgAl–CO_3$ | 11.35 | 7.79 | 0 0 3 |
| | 22.66 | 3.92 | 0 0 6 |
| | 34.46 | 2.60 | 0 0 9 |
| | 60.25 | 1.53 | 1 1 0 |
| $NiMgAl–CO_3$ | 11.37 | 7.77 | 0 0 3 |
| | 22.60 | 3.93 | 0 0 6 |
| | 34.34 | 2.61 | 0 0 9 |
| | 60.40 | 1.53 | 1 1 0 |
| $CuMgAl–CO_3$ | 11.26 | 7.85 | 0 0 3 |
| | 22.77 | 3.90 | 0 0 6 |
| | 34.69 | 2.58 | 0 0 9 |
| | 60.13 | 1.53 | 1 1 0 |
| $MgAl–CO_3$ | 11.34 | 7.80 | 0 0 3 |
| | 22.83 | 3.89 | 0 0 6 |
| | 34.41 | 2.60 | 0 0 9 |
| | 60.41 | 1.53 | 1 1 0 |
| MgAl–CoY | 11.35 | 7.79 | 0 0 3 |
| | 22.59 | 3.93 | 0 0 6 |
| | 34.41 | 2.60 | 0 0 9 |
| | 60.41 | 1.53 | 1 1 0 |
| MgAl–NiY | 6.70 | 13.17 | 0 0 3[a] |
| | 11.35 | 7.79 | 0 0 3 |
| | 12.53 | 7.06 | 0 0 6[a] |
| | 19.10 | 4.64 | 0 0 9[a] |
| | 23.02 | 3.86 | 0 0 6 |
| | 34.26 | 2.61 | 0 0 9 |
| | 60.56 | 1.53 | 1 1 0 |
| MgAl–CuY | 7.25 | 12.18 | 0 0 3[a] |
| | 11.41 | 7.74 | 0 0 3 |
| | 14.55 | 6.08 | 0 0 6[a] |
| | 22.53 | 3.94 | 0 0 6 |
| | 34.48 | 2.60 | 0 0 9 |
| | 60.40 | 1.53 | 1 1 0 |

[a]Phase formed due to the intercalation of $MY^{2-}$ species into the intergallery space of LDH.

### 3.2. Incorporation of transition metals into Mg–Al LDH

Another feature that differentiates the two methods of LDH synthesis can be seen upon comparison of data obtained by XRF technique for metal content in the synthesized materials (Table 2). The traditional coprecipitation of metal cations with the carbonate counter-ion at pH = 10.0 produced LDHs with almost the same metal ratios as in the starting solution (i.e., *M*(II):Mg(II):Al(III) 1:6:2), which indicated the complete incorporation of transition metals. In contrast with these results, the content of transition metals in the LDHs prepared by pre-chelation with edta was found to be much lower, although the syntheses were performed with the same starting metal ratios as the traditional coprecipitation. It is seen that the efficiency of incorporation was about 44% for Co (as of $CoY^{2-}$) and 47% for Ni and Cu. At the same time, the Mg–Al ratio for those three samples remained almost unchanged (i.e., 6:2). This suggested that—in order to properly balance the positive charges of the brucite-like layers—the LDH, synthesized via pre-chelation of transition metals, ought to involve some other anions present in the solution. These could most probably be the nitrate (from the starting metal salts) and carbonate that would originate from $CO_2$ in air. One should not also exclude the opportunity for hydroxide anions ($OH^-$) to play this role, as it is known to occur in a natural mineral of meixnerite $[Mg_6Al_2(OH)_{16}](OH)_2 \cdot 4H_2O$ [10–13].

### 3.3. Thermal behavior of materials

The results of thermal analysis of the synthesized LDH are presented in Fig. 3 and Table 4. All the synthesized LDH exhibited a two-step decomposition upon heating under the inert atmosphere of helium. The first step occurred at temperatures up to 220–240 °C and accounted for a 6.6–15.0% weight loss due to the desorption of physisorbed water ($m/z = 18$) and carbon dioxide ($m/z = 44$) and to the release of structural water. The second step took place at 350–500 °C, which was due to LDH dehydroxylation (forming water as product) and decomposition of incorporated anions. The observed loss in sample weight was about 42% for conventionally synthesized LDH and more than 48% for materials prepared via pre-chelation of transition metals with edta. An interesting feature can be seen upon comparison of differential thermogravimetry (DTG) profiles for *M*(II) $MgAl–CO_3$ LDH (Fig. 3A*–D*). Although the amount of carbonate anions used in the synthesis of LDH was 2.5 times higher than that required by stoichiometry (Table 2), the competitive incorporation of nitrate anions into LDH occurred. Decomposition of nitrate produced nitrogen monoxide (NO; $m/z = 30$) that was monitored in the effluent gases by MSD. The higher temperature (547 °C) was required for decomposing $NO_3^-$ in a reference hydrotalcite (D*). For transition metal-containing LDH, two peaks of NO formation were clearly observed. The peak at higher temperature could be associated with the decomposition of intercalated $NO_3^-$ as it occurred in the $MgAl–CO_3$ hydrotalcite. The peak at lower temperature could be assigned to decomposition of $NO_3^-$ associated with the transition metals. It should be noticed that incorporation of transition metals facilitates the thermal decomposition of nitrate. As seen in Fig. 3 for *M*(II) $MgAl–CO_3$ LDH, the NO from both kinds of $NO_3^-$ was formed at lower temperatures than that from the reference hydrotalcite.

The thermal behavior of MgAl–*M*Y LDH exhibited some interesting features as well. As mentioned above, such LDH experienced a much higher weight loss in step 2 (48.2–50.5% vs. about 42% for *M*(II)$MgAl–CO_3$) that was due to the decomposition of edta chelate involved. Monitoring of effluent gases by MSD for $m/z = 14$ (i.e., $CH_2$ fragments) and for $m/z = 28$ ($CH_2CH_2$) revealed that under inert atmosphere the process of chelate decomposition was more complicated and needed a higher temperature than that for decomposition of carbonate and nitrate. In DTG profiles (Fig. 3E*–G*), the peaks due to the

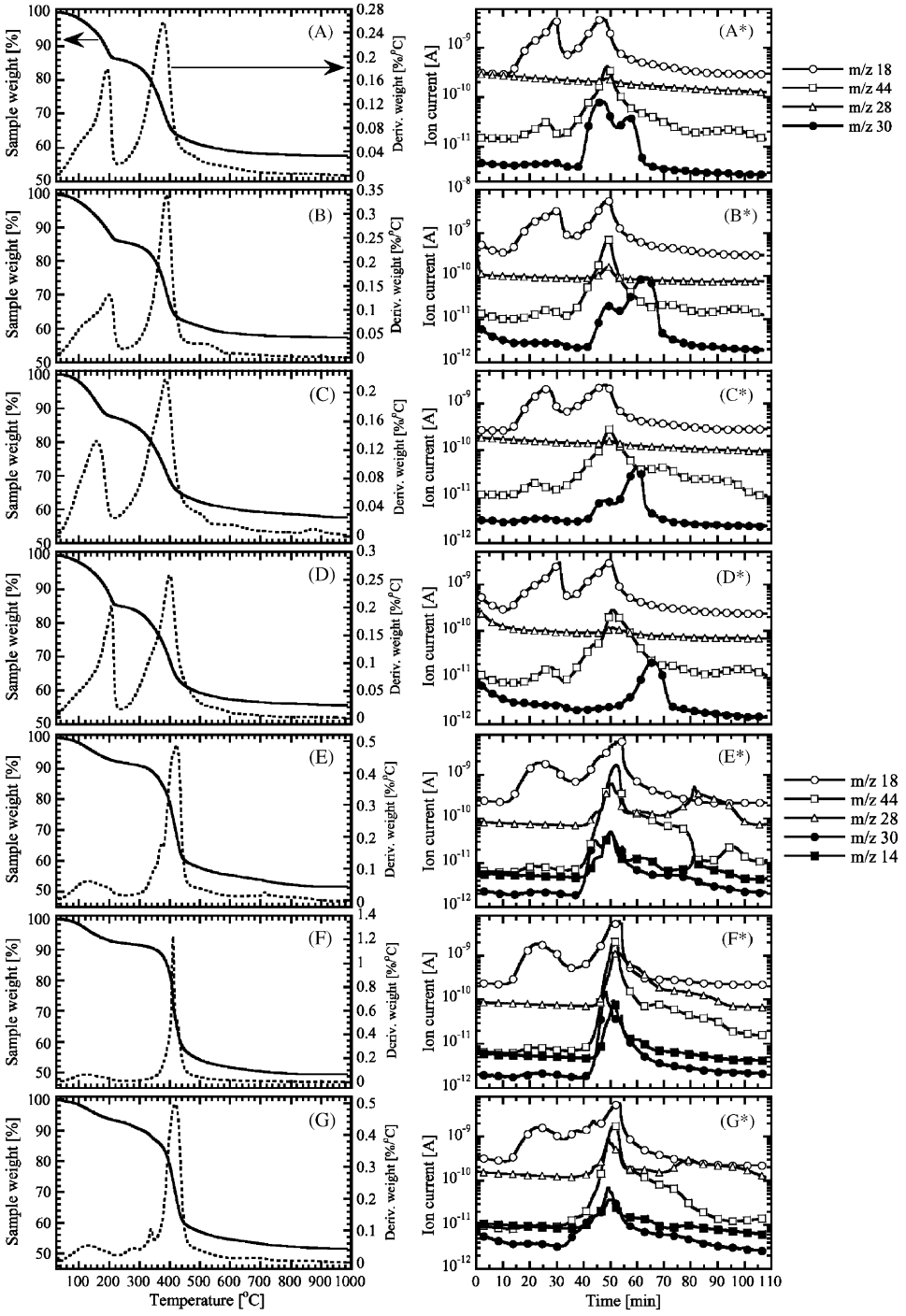


Fig. 3. Thermal behavior of Mg–Al LDH and identification of their decomposition products by selective ion monitoring of effluent gases with MSD: CoMgAl–$CO_3$ (A, A*), NiMgAl–$CO_3$ (B, B*), CuMgAl–$CO_3$ (C, C*), MgAl–$CO_3$ (D, D*), MgAl–CoY (E, E*), MgAl–NiY (F, F*) and MgAl–CuY (G, G*).

formation of $CO_2$ ($m/z = 44$) were more intense than that of hydrotalcite (D*), because the edta chelate had four carboxylic functional groups per molecule (Scheme 1). Formation of NO ($m/z = 30$) was also observed while these MgAl–*M*Y LDHs were decomposed. However, it was not possible to clearly differentiate the sources of NO that could originate from decomposition of impurity $NO_3^-$ and from two nitrogen atoms of edta ligand.

### 3.4. Vibrational spectroscopy studies

The use of a LabRam-IR HR800 system, which combined a miniaturized FTIR interferometer with a high-resolution dispersive Raman spectrometer equipped with a confocal microscope into one apparatus, offered unique opportunity to collect FTIR and Raman spectra from almost the same areas of the samples without any

Table 4
Thermal analysis of Mg–Al double hydroxides

| Material (loading in mg) | Loss in weight (%) | | | DTG profile | Thermal processes identified |
|---|---|---|---|---|---|
| | Step 1 | Step 2 | Total | | |
| CoMgAl–$CO_3$ (77.2) | 13.8 | 28.6 | 42.4 | 113 °C$^{(sh)}$, 192 °C$^{(p)}$<br>379 °C$^{(p)}$<br>470 °C$^{(sh)}$ | Release of physisorbed $H_2O$ and $CO_2$, removal of structural $H_2O$<br>LDH dehydroxylation, decomposition of $CO_3^{2-}$ and $NO_3^-$<br>Decomposition of $NO_3^-$ |
| NiMgAl–$CO_3$ (97.6) | 14.0 | 28.3 | 42.3 | 132 °C$^{(sh)}$, 199 °C$^{(p)}$<br>390 °C$^{(p)}$<br>514 °C$^{(sh)}$ | Release of physisorbed $H_2O$ and $CO_2$, removal of structural $H_2O$<br>LDH dehydroxylation, decomposition of $CO_3^{2-}$ and $NO_3^-$<br>Decomposition of $NO_3^-$ |
| CuMgAl–$CO_3$ (59.3) | 12.8 | 29.6 | 42.4 | 158 °C$^{(p)}$<br>387 °C$^{(p)}$<br>500 °C$^{(sh)}$ | Release of physisorbed $H_2O$ and $CO_2$, removal of structural $H_2O$<br>LDH dehydroxylation, decomposition of $CO_3^{2-}$ and $NO_3^-$<br>Decomposition of $NO_3^-$ |
| MgAl–$CO_3$ (63.7) | 15.0 | 29.3 | 44.3 | 206 °C$^{(p)}$<br>400 °C$^{(p)}$<br>547 °C$^{(sh)}$ | Release of physisorbed $H_2O$ and $CO_2$, removal of structural $H_2O$<br>LDH dehydroxylation, decomposition of $CO_3^{2-}$<br>Decomposition of $NO_3^-$ |
| MgAl–CoY (123.6) | 8.3 | 40.1 | 48.4 | 131 °C$^{(p)}$<br>373 °C$^{(sh)}$, 423 °C$^{(p)}$<br>715 °C$^{(p)}$ | Release of physisorbed $H_2O$ and $CO_2$, removal of structural $H_2O$<br>LDH dehydroxylation, decomposition of edta chelate<br>Decomposition of edta chelate |
| MgAl–NiY (123.9) | 8.0 | 42.5 | 50.5 | 124 °C$^{(p)}$<br>412 °C$^{(p)}$, 423 °C$^{(sh)}$ | Release of physisorbed $H_2O$ and $CO_2$, removal of structural $H_2O$<br>LDH dehydroxylation, decomposition of edta chelate |
| MgAl–CuY (124.9) | 6.6 | 41.6 | 48.2 | 130 °C$^{(p)}$<br>278 °C$^{(sh)}$, 338 °C$^{(p)}$<br>418 °C$^{(p)}$ | Release of physisorbed $H_2O$ and $CO_2$, removal of structural $H_2O$<br>Partial LDH dehydroxylation, decomposition of $NO_3^-$<br>LDH dehydroxylation, decomposition of edta chelate |

$^{(sh)}$DTG peak shoulder; $^{(p)}$DTG peak.

special pretreatments [14]. For acquiring FTIR spectra, the powdered samples were brought into contact with a ZnSe/diamond crystal of an ATR objective. The FTIR spectra of Mg–Al LDHs prepared by two different techniques are shown in Fig. 4. Also shown for comparison is the spectrum of the reference MgAl–$CO_3$ hydrotalcite. One can certainly see the difference in spectra of the LDH prepared by the traditional coprecipitation technique and those involving the pre-chelation of transition metals with edta. The $M$(II)MgAl–$CO_3$ LDH ($M$ = Co, Ni, Cu) exhibited similar spectra to each other and to the reference hydrotalcite. The most intense peak observed was around 1360–1366 $cm^{-1}$ and corresponded to the antisymmetric stretching mode ($\nu_3$) of carbonate and nitrate anions residing in the interlayer space of LDH (Table 5). The symmetrical stretching vibration ($\nu_1$) of these anions appeared as a weak peak around 1039–1043 $cm^{-1}$. Medium in intensity and broad peak in a 1614–1634 $cm^{-1}$ range appeared to be due to the bending (deformation) mode of water molecules also present in the synthesized materials. The stretching vibrations of OH and water molecules appeared as a group of the overlapping two or three peaks with maxima around 3464–3501 $cm^{-1}$. All spectra thus obtained were in full agreement with those reported in the literature [15]. The FTIR spectra collected for MgAl–$M$Y LDH ($M$ = Co, Ni, Cu) differed significantly from those described above. The presence of edta chelates of transition metals in the LDH led to the appearance of new peaks and shoulders in the FTIR spectra. A strong and almost symmetric peak around 1586–1595 $cm^{-1}$ was assigned to the stretching of $COO^-$ groups coordinated to transition metal cations (Scheme 1). The absence of an additional peak or shoulder at higher wavenumbers (up to 1630 $cm^{-1}$) indicated that the metal chelates did not have free (i.e., non-coordinated) ionized $COO^-$ group(s) and all four carboxylic functional groups of $edta^{4-}$ were equivalently coordinated to transition metal cations [16–20]. A group of weak peaks around 2926–2972 $cm^{-1}$ arose due to C–H stretching of the $CH_2$ groups of edta. Two peaks in the range of 1083–1117 $cm^{-1}$ were ascribed to C–N stretching while a peak shoulder at 1271–1275 $cm^{-1}$ could be assigned to the stretching of C–C (i.e., $CH_2$–COO) bonds [21,22].

For acquiring Raman spectra, the synthesized samples were irradiated with an Ar-ion laser light. One should here mention that the LDHs had different stability against heating due to laser irradiation. All materials prepared by traditional coprecipitation of metal cations and carbonate (i.e., $M$(II)MgAl–$CO_3$) were found to sustain heating without deterioration and were analyzed using the original power of laser, i.e., without using filters to decrease the power delivered to a specimen. On the contrary, the LDH containing chelated transition metals were notably damaged after direct irradiation with full intensity laser light (i.e., 20 mW at laser head): one could observe using the microscope that after analysis some specimens became "punched" by the laser beam and had a hole in the area

where the laser light was focused prior to the spectrum acquisition. This made it necessary to reduce the energy input to a half or a quarter of the original value by using suitable filters on the trajectory of the laser beam prior to reaching the specimen. Raman spectra obtained for $M$(II)MgAl–$CO_3$ LDHs and the reference hydrotalcite are shown in Fig. 5. All spectra showed sharp, intense peaks around 1047 and 1060 $cm^{-1}$ that could be assigned to symmetric stretching vibrations ($v_1$) of incorporated nitrate and carbonate anions (Table 6) [23]. Other spectra features included two peaks around 474 and 545 $cm^{-1}$ that could be due to "Al/Mg"–OH translation, a broad peak of low intensity at 1390 $cm^{-1}$ due to antisymmetric stretching vibrations ($v_3$) of interlayer carbonate and nitrate anions, and the overlapping peaks around 3500–3600 $cm^{-1}$ attributed to the stretching vibrations of OH and water molecules [24]. The Raman spectra of MgAl–$M$Y LDH are presented in Fig. 6. Also shown for comparison are the spectra of solid sodium edetates $Na_2MY \cdot xH_2O$ ($M$ = Co, Ni, Cu). The presence of sharp, intense peaks at 1044 $cm^{-1}$ with a shoulder at 1059 $cm^{-1}$ in the LDH spectra indicated that all materials contained $NO_3^-$ and $CO_3^{2-}$ anions (Table 6). Incorporation of edta chelates of transition metals into the LDH was confirmed by the appearance of a group of intense peaks around 2852–2954 $cm^{-1}$ that were assigned to symmetric and antisymmetric C–H stretching vibrations of the $CH_2$ groups of edta chelate [25]. The symmetric peaks at 918–921 $cm^{-1}$ appeared to be due to C–C (i.e., $CH_2$–COO) stretching vibrations of the chelate while peaks around 460–470 $cm^{-1}$ could be attributed to the stretching vibrations of coordination bonds between metal and two nitrogen atoms of edta (Scheme 1) [26–29]. It should be added that "Al/Mg"–OH translation vibrations could also contribute to the peak at 460–470 $cm^{-1}$ and the peak around 550–552 $cm^{-1}$ was supposed to be due to such mode as well.

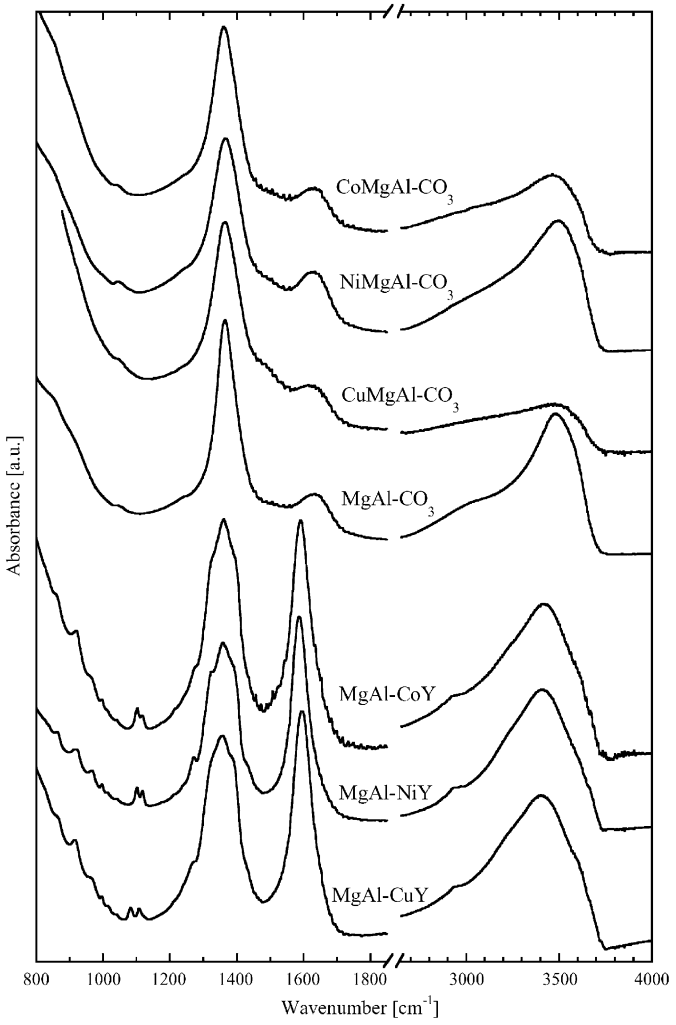


Fig. 4. FTIR spectra of Mg–Al layered double hydroxides containing transition metals (spectrum of the reference MgAl–$CO_3$ hydrotalcite is shown for comparison).

## 4. Discussion

While synthesis of LDH by coprecipitation of metal cations under basic conditions has been a well known and widely used procedure, the chelation of transition metals with $edta^{4-}$ to form stable anionic complexes prior to coprecipitation with Mg(II) and Al(III) is a more novel approach. The results of this work showed that LDHs synthesized by this technique differed significantly in their properties from those traditionally prepared. The integrity

Table 5
Infrared spectra peak ($cm^{-1}$) assignments for Mg–Al layered double hydroxides

| | CoMgAl–$CO_3$ | NiMgAl–$CO_3$ | CuMgAl–$CO_3$ | MgAl–$CO_3$ |
|---|---|---|---|---|
| Interlayer $CO_3^{2-}$ and $NO_3^-$ | 1040 ($v_1$), 1360 ($v_3$) | 1043 ($v_1$), 1366 ($v_3$) | 1040 ($v_1$), 1366 ($v_3$) | 1040 ($v_1$), 1360 ($v_3$) |
| $H_2O$ bending mode | 1634 | 1634 | 1614 | 1634 |
| OH and $H_2O$ stretching vibrations (overlapping peaks) | 3464 | 3500 | 3477 | 3464 |
| | MgAl–CoY | MgAl–NiY | | MgAl–CuY |
| C–N stretching | 1103, 1116 | 1101, 1117 | | 1083, 1108 |
| C–C (i.e., $CH_2$–COO) stretching | 1275 | 1271 | | 1271 |
| $COO^-$ stretching | 1591 | 1586 | | 1595 |
| C–H stretching of the $CH_2$ groups | 2926, 2966 | 2931, 2937, 2960, 2972 | | 2940, 2968 |
| OH and $H_2O$ stretching vibrations (overlapping peaks) | 3410 | 3402 | | 3402 |

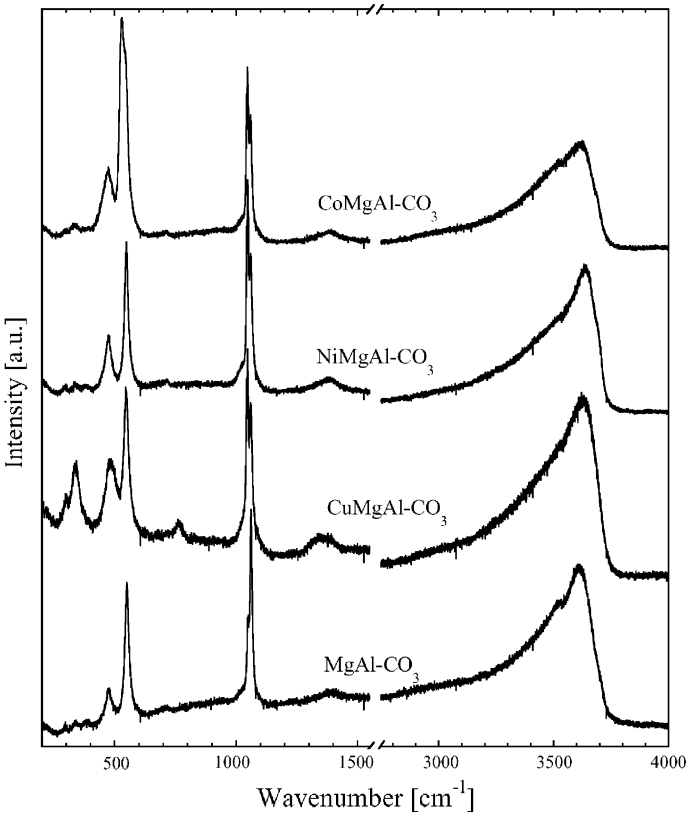


Fig. 5. Raman spectra of $M$(II)MgAl–$CO_3$ LDH synthesized by conventional coprecipitation technique (spectrum of the reference MgAl–$CO_3$ hydrotalcite is shown for comparison).

Table 6
Raman spectra peak ($cm^{-1}$) assignments for Mg–Al layered double hydroxides

| | CoMgAl–$CO_3$ | NiMgAl–$CO_3$ | CuMgAl–$CO_3$ | MgAl–$CO_3$ |
|---|---|---|---|---|
| "Al/Mg"–OH translation | 474, 530, 545$^{(sh)}$ | 474, 548 | 480, 545 | 477, 550 |
| Interlayer $CO_3^{2-}$ | 1059 ($v_1$) | 1059 ($v_1$) | 1060 ($v_1$) | 1064 ($v_1$) |
| Interlayer $NO_3^-$ | 1046 ($v_1$) | 1047 ($v_1$) | 1047 ($v_1$) | 1049 ($v_1$) |
| Interlayer $CO_3^{2-}$ and $NO_3^-$ | 1392 ($v_3$) | 1387 ($v_3$) | 1341, 1378 ($v_3$) | 1411 ($v_3$) |
| OH and $H_2O$ stretching vibrations (overlapping peaks) | 3524, 3624 | 3631 | 3620 | 3524, 3613 |

| | MgAl–CoY | MgAl–NiY | MgAl–CuY |
|---|---|---|---|
| "Al/Mg"–OH translation | 463, 552 | 470, 550 | 469, 550 |
| N–M stretching | 463 | 470 | 469 |
| C–C (i.e., $CH_2$–COO) stretching | 919 | 918 | 921 |
| Interlayer $NO_3^-$ | 1044 ($v_1$) | 1043 ($v_1$) | 1044 ($v_1$) |
| Interlayer $CO_3^{2-}$ | 1060$^{(sh)}$ ($v_1$) | 1059$^{(sh)}$ ($v_1$) | 1059$^{(sh)}$ ($v_1$) |
| C–H stretching of the $CH_2$ groups | 2872, 2911, 2928, 2951 | 2878, 2914, 2931, 2954 | 2852, 2942 |
| OH and $H_2O$ stretching vibrations (overlapping peaks) | 3490, 3634, 3680 | 3465, 3631, 3678 | 3436, 3626, 3674 |

$^{(sh)}$Peak shoulder.

and coordination state of metal chelates upon incorporation into the LDH structure was of particular interest. Several changes could be expected due to the chemistry involved. It was reported in the literature that in aqueous solutions the edta chelate may change its coordination state from hexadentate to pentadentate if water molecule replaces one of four ionized carboxylic groups coordinated to the transition metal (Scheme 2) [30]. This does not change the total charge of the metal complex but leads to the appearance of uncoordinated ("free") ionized carboxylic groups. In our studies, when reaction was carried out in the heated solution and the concentration of hydroxide ions in solution was moderately high (pH = 10.5), one would also expect the substitution of coordinated water molecule with hydroxide anion leading to the change of the total charge of chelate to (−3)

(Scheme 3). The results of FTIR spectroscopy studies showed that all four ionized carboxylic groups were equivalently coordinated to transition metal cations. The presence of a single symmetric peak at 918–921 $cm^{-1}$ in Raman spectra due to C–C (i.e., $CH_2$–COO) stretching vibrations also confirmed that all four $COO^-$ groups were equivalent to each other. Otherwise this peak would split or a shoulder would appear. To sum up, these observations clearly indicated that the structure of edta chelates of transition metals was preserved upon incorporation into the Mg–Al LDH.

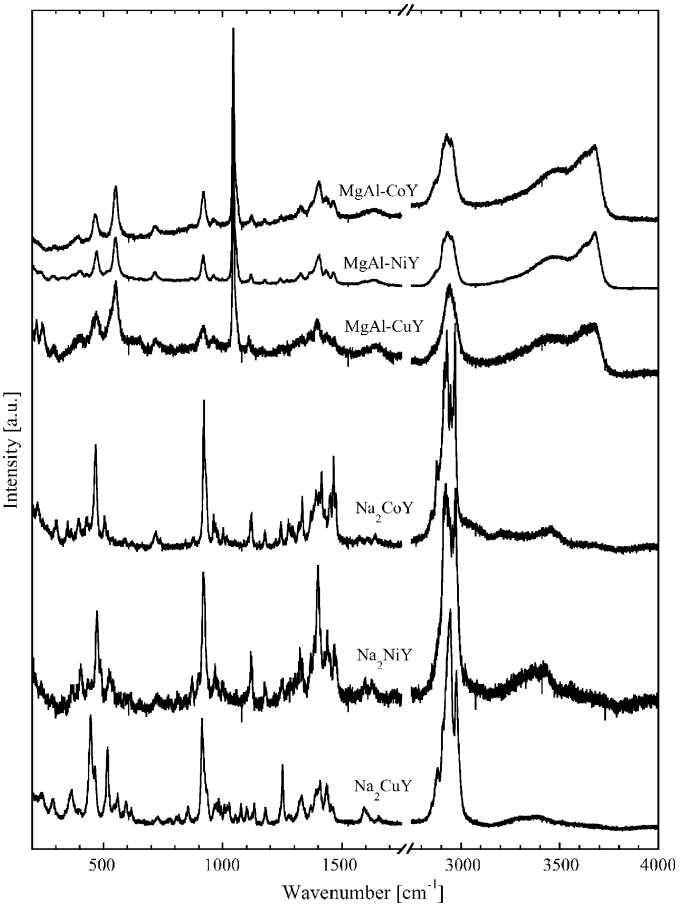


Fig. 6. Raman spectra of Mg–Al LDH containing edta chelates of transition metals (also shown for comparison are the spectra of solid edetates $Na_2MY$ ($M$ = Co, Ni, Cu)).

## 5. Conclusion

Two methods of synthesizing Mg–Al LDH containing Co, Ni and Cu were compared. The traditional coprecipitation of metal cations under basic conditions produced LDHs very similar in structure and properties to those of synthetic hydrotalcite. The metal content in the LDH products measured by XRF corresponded to that in the starting solutions, which indicated the complete incorporation of transition metals into the LDH upon coprecipitation. Although the carbonate counter-ion was used for synthesis in considerable excess with respect to the amount required by the reaction stoichiometry, incorporation of nitrate into $M$(II)MgAl–$CO_3$ also occurred as demonstrated by TG-MSD and vibrational spectroscopy. The alternative technique was based on the pre-chelation of transition metals with $edta^{4-}$ followed by coprecipitation of such metal chelates with Mg(II) and Al(III). The LDH prepared by this technique revealed XRD patterns similar to that of hydrotalcite. However, for MgAl–NiY and MgAl–CuY materials, additional layered phases with larger d-spacings were detected. This suggested that $MY^{2-}$ species intercalated the intergallery space of Mg–Al LDH thus forming the new and stable lamellar phases. The efficiency of transition metal incorporation varied from 44% for $CoY^{2-}$ to 47% for $NiY^{2-}$ and $CuY^{2-}$. FTIR and Raman spectroscopy studies provided evidence that the

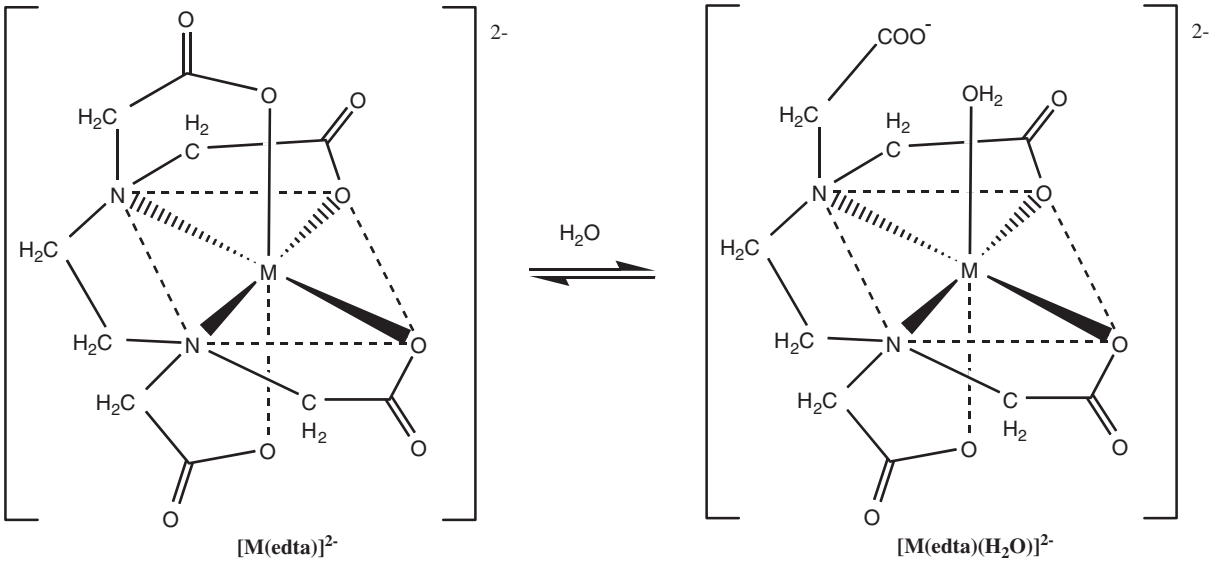


Scheme 2.

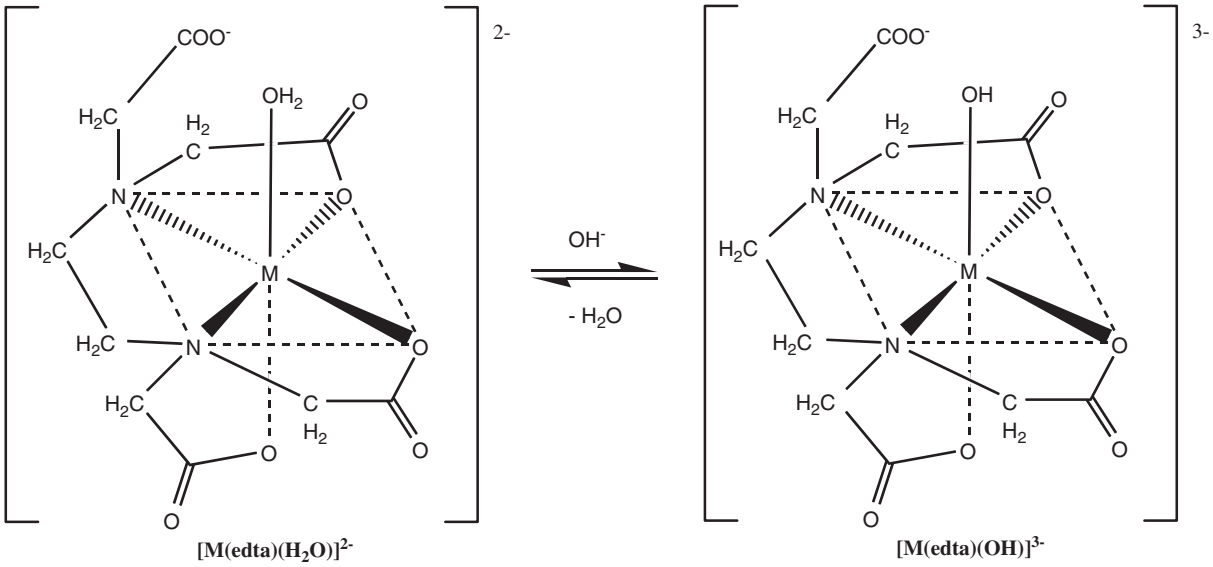


Scheme 3.

metal chelates maintained their integrity upon incorporation into the LDH.

## Acknowledgments

The generous financial support of the Natural Sciences and Engineering Council of Canada (NSERC) and the Ontario Research & Development Challenge Fund (ORDCF) is acknowledged. A.S. thanks the Canadian Government for a Canada Research Chair in Catalysis by Nanostructured Materials (2001–2008). Thanks are due to Mr. J. Ronald Hartree (Department of Earth Sciences) and Dr. Peter J.E. Harlick (CCRI) for their help with XRF and TG-MSD analyses of samples.

## References

[1] V. Rives, Layered Double Hydroxides: Present and Future, NOVA Science, New York, 2001.
[2] F. Trifiro, A. Vaccari, in: G. Alberti, T. Bein (Eds.), Solid-State Supramolecular Chemistry: Two- and Three-Dimensional Inorganic Networks, Pergamon Press, Exeter, 1996, pp. 251–291 (Chapter 8).
[3] F. Cavani, F. Trifiro, A. Vaccari, Catal. Today 11 (1991) 173–301.
[4] A. Vaccari, Catal. Today 41 (1998) 53–71.
[5] B.F. Sels, D.E. De Vos, P.A. Jacobs, Catal. Rev. Sci. Eng. 43 (2001) 443–488.
[6] K. Takehira, Catal. Surv. Japan 6 (2002) 19–32.
[7] J.A. Dean, Lange's Handbook of Chemistry, McGraw-Hill, New York, 1992, p. 8.93.
[8] A.I. Tsyganok, K. Suzuki, S. Hamakawa, K. Takehira, T. Hayakawa, Chem. Lett. 30 (2001) 24–25.
[9] A.I. Tsyganok, K. Suzuki, S. Hamakawa, K. Takehira, T. Hayakawa, Catal. Lett. 77 (2001) 75–86.
[10] S.K. Yun, V.R.L. Constantino, T.J. Pinnavaia, Clays Clay Miner. 43 (1995) 503–510.
[11] D. Tichit, M.N. Bennani, F. Figueras, R. Tessier, J. Kervennal, Appl. Clay Sci. 13 (1998) 401–415.
[12] F. Prinetto, G. Ghiotti, R. Durand, D. Tichit, J. Phys. Chem. B 104 (2000) 11117–11126.
[13] J.J. Bravo-Suarez, E.A. Paez-Mozo, S.T. Oyama, Chem. Mater. 16 (2004) 1214–1225.
[14] F. Adar, G. LeBourdon, J. Reffner, A. Whitley, Spectroscopy 18 (2003) 34–40.
[15] J.T. Kloprogge, R.L. Frost, in: V. Rives (Ed.), Layered Double Hydroxides: Present and Future, NOVA Science, New York, 2001, pp. 139–192 (Chapter 5)(and references therein).
[16] D.H. Busch, J.C. Bailar, J. Am. Chem. Soc. 75 (1953) 4574–4575.
[17] D.H. Busch, J.C. Bailar, J. Am. Chem. Soc. 78 (1956) 716–719.
[18] M.L. Morris, D.H. Busch, J. Am. Chem. Soc. 78 (1956) 5178–5181.
[19] G. Socrates, Infrared and Raman Characteristic Group Frequencies: Tables and Charts, Wiley, Chichester, 2001 (Chart 22.3, pp. 295–298).
[20] K. Nakamoto, Infrared and Raman Spectra of Inorganic and Coordination Compounds (Part B: Applications in Coordination, Organometallic, and Bioinorganic Chemistry), Wiley-Interscience, New York, 1997 (Chapter III-9, pp. 62–69).
[21] D.T. Sawyer, P.J. Paulsen, J. Am. Chem. Soc. 81 (1959) 816–820.
[22] R.E. Sievers, J.C. Bailar, Inorg. Chem. 1 (1962) 174–182.
[23] K. Nakamoto, Infrared and Raman Spectra of Inorganic and Coordination Compounds (Part A: Theory and Applications in Inorganic Chemistry), Wiley-Interscience, New York, 1997 (Chapter II-4, pp. 180–184).
[24] J.T. Kloprogge, L. Hickey, R.L. Frost, J. Raman Spectrosc. 35 (2004) 967–974.
[25] K. Nakamoto, Infrared and Raman Spectra of Inorganic and Coordination Compounds (Part A: Theory and Applications in Inorganic Chemistry), Wiley-Interscience, New York, 1997 (Chapter I-18, pp. 88–95).
[26] K. Krishnan, R.A. Plane, J. Am. Chem. Soc. 90 (1968) 3195–3200.
[27] R.H. Nuttall, D.M. Stalker, Inorg. Nucl. Chem. Lett. 12 (1976) 639–641.
[28] E. Faulques, D.L. Perry, S. Lott, J.D. Zubkowski, E.J. Valente, Spectrochim. Acta A 54 (1998) 869–878.
[29] E.J. Baran, C.C. Wagner, M.H. Torre, J. Braz. Chem. Soc. 13 (2002) 576–582.
[30] M.W. Grant, H.W. Dodgen, J.P. Hunt, J. Am. Chem. Soc. 93 (1971) 6828–6831.